ENVIRONMENTAL ENGINEERING SCIENCE
Volume 34, Number 10, 2017

DOI: 10.1089/ees.2016.0464

Reduction in Chemical Oxygen Demand of TNT Red Water Using Layered Double Hydroxide Prepared from Red Mud and Brucite

Pan Hu,[1] Yihe Zhang,[1,*] Fengzhu Lv,[1,*] Xinke Wang,[1] Wangshu Tong,[1]
Zilin Meng,[1] Paul K. Chu,[2] and Anzhen Zhang[1]

[1]*Beijing Key Laboratory of Materials Utilization of Nonmetallic Minerals and Solid Wastes, National Laboratory of Mineral Materials, School of Materials Science and Technology, China University of Geosciences, Beijing, China.*
[2]*Department of Physics and Materials Science, City University of Hong Kong, Tat Chee Avenue, Kowloon, Hong Kong, China.*

Received: September 15, 2016 Accepted in revised form: February 18, 2017

Abstract

A low-cost organolayered double hydroxide adsorbent prepared under alkali conditions with red mud (waste tailings from alumina production) and brucite is modified by anionic surfactant, sodium dodecyl benzene sulfonate (SDBS), by ion exchange to produce a layered double hydroxide adsorbent (LDH-SDBS). LDH-SDBS was used to treat 2,4,6-trinitrotoluene (TNT) red water that had high toxicity, contained persistent compounds, and had a high chemical oxygen demand (COD). Removal efficiency reached 46% at 20-fold dilution (COD, 4024 mg/L) and kinetics showed that adsorption processes followed a pseudo-second-order model. Negative ΔG and positive ΔH indicated adsorption was spontaneous and endothermic and Gas Chromatography-Mass Spectrometer (GC/MS) revealed that amounts of organic compounds in TNT red water were reduced significantly.

Keywords: adsorption; brucite; layered double hydroxides; red mud; TNT red water

Introduction

The 2,4,6-trinitrotoluene (TNT) explosive, a nitroaromatic compound, is one of the most important products in military and civilian industrial production. According to the conventional production process, which is typically based on complete nitration of toluene, crude TNT is purified by water and sodium sulfite baths leading to two types of wastewater: yellow water and red water (Ayoub *et al.*, 2010). TNT red water produced during purification of crude TNT by sodium sulfite is a dark red and hazardous solution containing dissolved dinitrotoluene sulfonates (mainly 2,4-dinitrotoluene-3-sulfonate and 2,4-dinitrotoluene-5-sulfonate), trinitrotoluene, nitrotoluene, dinitrotoluene, as well as other chemicals (Nefso *et al.*, 2005).

Several methods have been proposed to remove TNT and other organic species from wastewater, for example, adsorption (Zhang *et al.*, 2014), vacuum distillation (Zhao *et al.*, 2010), degradation utilizing microorganisms (Park *et al.*, 2003; Zhang *et al.*, 2015), oxidation by UV/H_2O_2 (Hwang *et al.*, 2004), Fenton reagent oxidation (Matta *et al.*, 2008), and photocatalytic oxidation (Zhu *et al.*, 2011; Shen *et al.*, 2014; Ludwichk *et al.*, 2015; Jo *et al.*, 2014). It has been suggested that adsorption is the most effective and practical method of TNT red water removal and many adsorbents have been used to treat TNT red water, for instance, active carbon (Wei *et al.*, 2011), active coke (Zhang *et al.*, 2011; Hu *et al.*, 2014, 2015), bamboo charcoal (Fu *et al.*, 2012), and macroporous polystyrene (Meng *et al.*, 2012, 2013; Zhao *et al.*, 2013). However, to our knowledge, removal of organic materials in TNT red water by adsorption to layered double hydroxides (LDHs) has not been reported to date.

The structural formula of LDH is shown as the general formula $[M^{II}_{1-x}M^{III}_{x}(OH)_2]^{x+}[A^{n-}_{x/n} \cdot mH_2O]^{x-}$, where M^{II} = Zn, Mg, Co, Ni, etc., M^{III} = Al, Fe, Cr, Ga, etc., and $A^{n-} = CO_3^{2-}$, NO_3^-, Cl^-, SO_4^{2-}, etc. This is a layered substance containing positively charged metal hydroxide sheets compensated by a large number of exchangeable charge-balancing anions and water molecules in the interlayer space (Braterman *et al.*, 2004). Owing to the presence of large interlayer spaces and a huge number of exchangeable anions, LDHs are good ion exchangers/adsorbents for the removal of toxic anions from waste water. Therefore, LDHs can be used to absorb the organics in TNT red water.

Several methods can be used to prepare LDHs. The most common method is coprecipitation at constant pH followed by aging at a certain temperature (Basile *et al.*, 1998). Urea is usually used as the base source to produce large LDH-CO_3

**Corresponding authors:* Yihe Zhang, Beijing Key Laboratory of Materials Utilization of Nonmetallic Minerals and Solid Wastes, National Laboratory of Mineral Materials, School of Materials Science and Technology, China University of Geosciences, Beijing 100083, China. *Phone:* +86 010-82322104; *Fax:* +86 010-82322104; *E-mail:* zyh@cugb.edu.cn *or* Fengzhu Lv, Beijing Key Laboratory of Materials Utilization of Nonmetallic Minerals and Solid Wastes, National Laboratory of Mineral Materials, School of Materials Science and Technology, China University of Geosciences, Beijing 100083, China. *Phone:* +86 010-82322104; *Fax:* +86 010-82322104; *E-mail:* lfz619@cugb.edu.cn

crystallites, which form hexagonal platy sheets by homogeneous precipitation (Evans and Slade, 2006). Reconstruction from MgAl oxide generated by calcining MgAl-CO_3 LDH at a mild temperature (e.g., 500°C) takes advantage of LDH ''memory'' effect in preparation of LDHs intercalated with desirable anions, including various inorganic, organic, and biomedical anions (Bontchev *et al.*, 2003; Nakayama *et al.*, 2004). Zhiping Xu *et al.* have prepared LDH from mixed MgO and Al_2O_3 (Zhi and Guo 2005). Stanimirova and Balek (2008) have characterized LDH Mg-Al-CO_3 prepared by rehydration of Mg-Al mixed oxide. In addition, mixed oxide derived from LDHs has been studied (Stanimirova and Balek 2008).

In this study, LDH is prepared with red mud and brucite that are industrial solid wastes residue and less expensive than laboratory reagents. Red mud, a solid waste with high pH (10–13) from the aluminum industry, contains fine particles mainly including gibbsite ($Al(OH)_3$), sodalite ($Na_4Al_3Si_3O_{12}Cl$), Muscovite ($KAl_2(AlSi_3O_{10})(OH)_2$), hematite ($Fe_2O_3$) and goethite ($\alpha$-FeOOH). For every ton of alumina produced, approximately one to two tons (dry weight) of bauxite residues are generated. The corrosive nature and enormous quantities (90 million tons yearly worldwide) of the red mud cause significant ecological problems and negative environmental impacts. Brucite selected in the study is industrial grade containing $Mg(OH)_2$, serpentine ($Mg_6[Si_4O_{10}]$ $(OH)_8$), magnesite ($MgCO_3$), and dolomite ($CaMg(CO_3)_2$). The calcined red mud and brucite contain abundant MgO, Al_2O_3 serving as the raw materials of LDH. LDH is used to treat the TNT red water, not only to reduce the chemical oxygen demand (COD) of TNT red water but also to realize recycling of solid waste.

Materials and Methods

Materials

Red mud was provided by Shandong Weiqiao Aluminum and Electricity Co. Ltd. (Shandong, China) and brucite was supplied by Kuandian brucite factory (Liaoning, China). The primary mineral components are shown in Table 1. TNT red water was supplied by Dongfang Chemical Corporation (Hubei, China). Sodium dodecyl benzene sulfonate (SDBS, Beijing Chemical Reagent Co.) and the other reagents used in this study were analytical grade and distilled water was used to prepare the solutions.

Adsorbent preparation

Red mud and brucite (1:2 mass ratio) were mixed with distilled water in a beaker and mixed thoroughly. The mixture was dried at 120°C, calcined at 600°C for 3 h, and air cooled to produce LDH dry powder.

The NaOH solution (1 M, 150 mL) and 150 mL of 2 M Na_2CO_3 solution were mixed with 60 g of LDH dry powder and the reaction proceeded at 30°C for 6 h. After aging for 24 h, the sample was filtrated and washed until the pH of filtrate reached 7. Then, it was dried at 80°C and milled to produce the LDH powder.

LDH powder (10 g) and 90 mL of distilled water were added to a beaker and stirred for 30 min. SDBS (3.6445 g) was dissolved in 40 mL of distilled water. It was added slowly to the mentioned suspension and stirred at room temperature for 24 h. The mixtures were filtrated and washed until the filtrate was

TABLE 1. PRIMARY MINERAL COMPONENTS OF RED MUD AND BRUCITE

Red mud	Mineral components	Muscovite ($KAl_2(AlSi_3O_{10})(OH)_2$)	Quartz (SiO_2)	Gibbsite ($Al(OH)_3$)	Calcite ($CaCO_3$)	Sodalite ($Na_8Al_6Si_6O_{24}(OH)_2$)	Hematite (Fe_2O_3)	Goethite (FeOOH)
	Content (wt%)	10	4	15	26	17	17	11
Brucite	Mineral components	Serpentine ($Mg_6[Si_4O_5](OH)_8$)	$Mg(OH)_2$	Magnesite ($MgCO_3$)	Dolomite ($CaMg(CO_3)_2$)			
	Content (wt%)	9	79	7	5			

neutral and no bubble was observed. The product was vacuum dried at 80°C for 12 h and milled to produce LDH-SDBS.

Adsorption experiments

Adsorption experiments were conducted using 4 g of LDH or LDH-SDBS as the adsorbent in a 100 mL flask containing 50 mL of TNT red water. The bottles were shaken in a digital water bath oscillator at 150 rpm. Then samples were filtered and dried under vacuum at 70°C for 8 h. The filtrate was analyzed by a COD rapid detector (5B-6, Lian-Hua Tech. Co., China) with a precision of ±5% to determine the adsorption efficiency. The relative removal of COD (%) of the organic compounds and q_e (mg/g) in the TNT red water adsorbed by LDH or LDH-SDBS were calculated based on Equations (1) and (2):

$$\text{Relative removal of COD } (\%) = \frac{COD_1 - COD_2}{COD_1} \times 100\%, \quad (1)$$

$$q_e = \frac{(COD_1 - COD_2)V}{W}, \quad (2)$$

where COD_1 (mg/L) and COD_2 are the COD of the initial TNT red water and treated red water after reaching equilibrium, respectively. V (L) is the volume of TNT red water and W (g) is the adsorbent weight. At any time, the amount of COD and the adsorbed q_e (mg/g) were calculated using a similar relationship based on Equation (2).

To determine the optimal contact time, the initial concentration of TNT red water, and temperature, adsorption experiments were performed systematically. TNT red water was diluted 0, 10, 20, 40, and 100 times, and the COD concentrations were 68,510, 9,454, 4,024, 2,964, and 660 mg/L, respectively.

Characterization

X-ray diffraction (XRD, Rigaku D/max-rA), scanning electron microscope (SEM, JSM-6301F), energy dispersive X-ray spectroscopy (EDS), thermogravimetric-differential thermal analysis (TG-DTA, Netzsch TG-209C), N_2 adsorption isotherm obtained a micrometric instrument (ASIQM0002-4), and Fourier transform infrared spectra (FT-IR, PerkinElmer Spectrum 100) were performed to characterize the structure, morphologies, and components of LDH or LDH-SDBS before and after adsorption.

Determination of compounds in TNT red water

A 6890N/5973 Gas Chromatography-Mass Spectrometer (GC/MS) system (Agilent Corporation) was used to determine the changes in the organic compounds in TNT red water before and after adsorption. The TNT red water samples were treated by liquid–liquid extraction using CH_2Cl_2 as the extractant (Li *et al.*, 2003). A sample with a volume of 1.0 μL was injected, operated from 40°C to 280°C at a programming rate of 2.0°C/min with the DB-35 MS capillary column (30 m × 0.25 mm × 0.25 μm). Pure helium gas was used as the carrier gas at a flow rate of 1.0 mL/min.

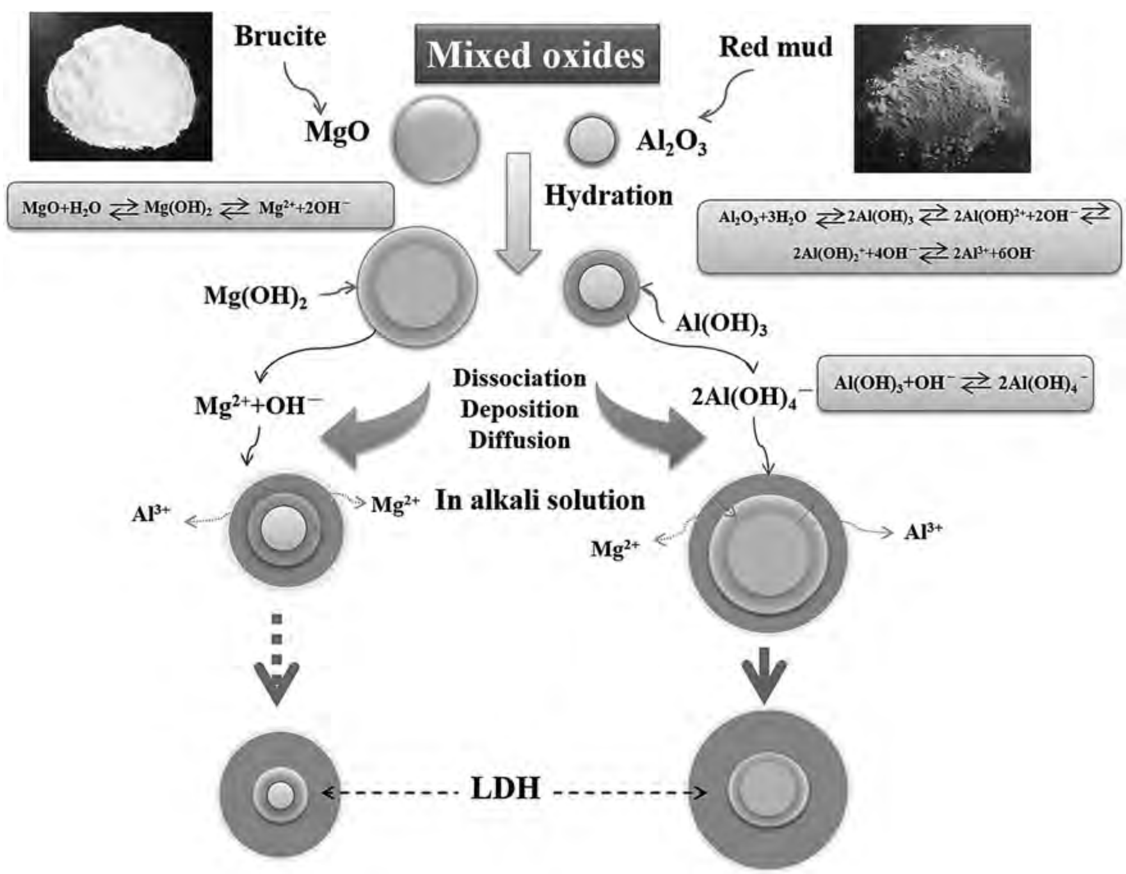

FIG. 1. Scheme for LDH preparation from red mud and brucite. LDH, layered double hydroxide.

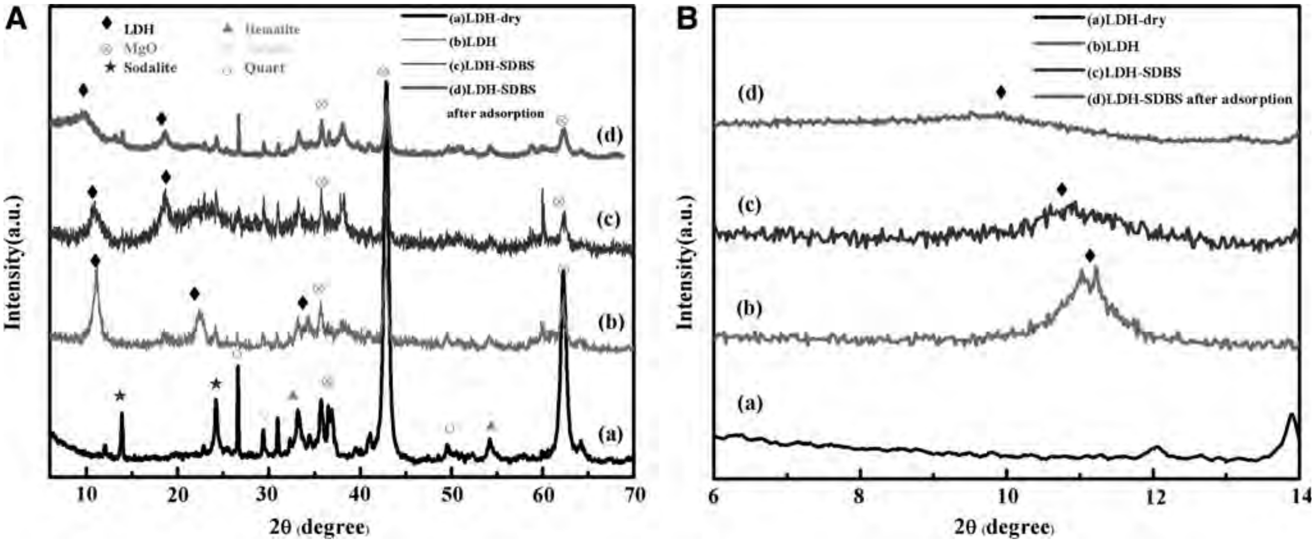

FIG. 2. (**A**) XRD patterns of (**a**) LDH dry powder, (**b**) LDH, (**c**) LDH-SDBS, and (**d**) LDH-SDBS after adsorption. (**B**) the low angle XRD patterns of (**a**) LDH dry powder, (**b**) LDH, (**c**) LDH-SDBS, and (**d**) LDH-SDBS after adsorption. LDH SDBS, layered double hydroxide-sodium dodecyl benzene sulfonate; XRD, X-ray diffraction.

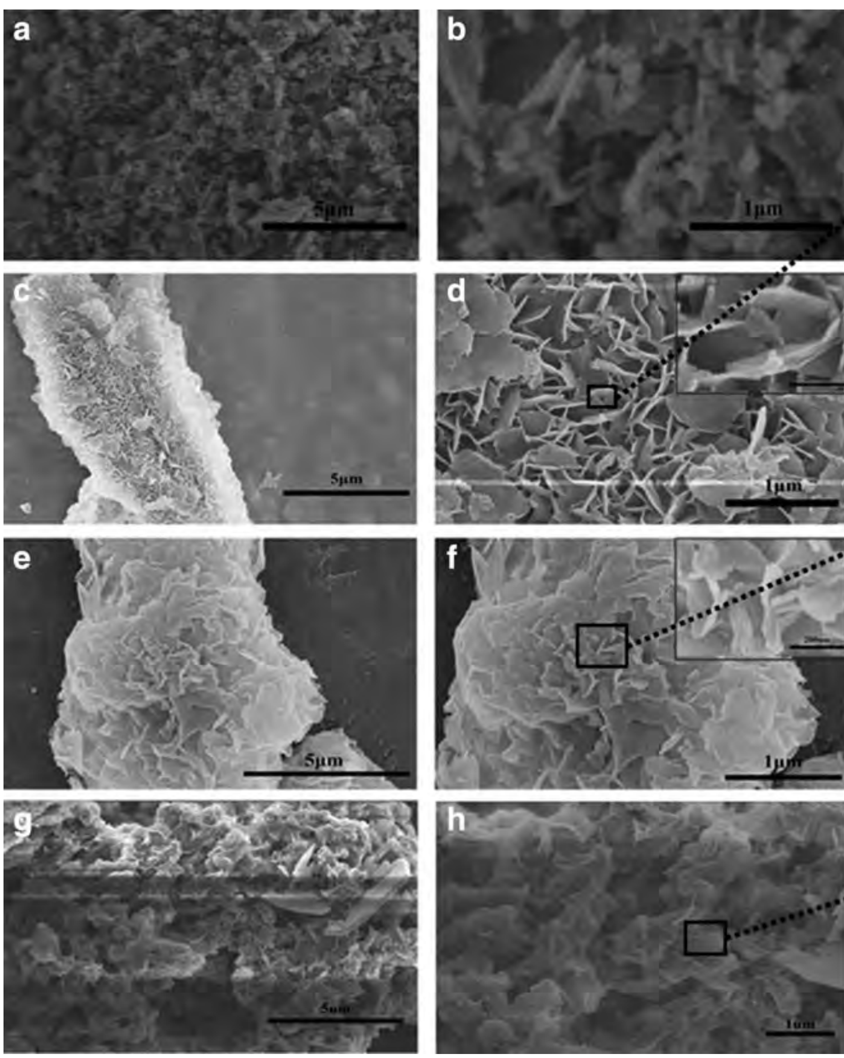

Element	wt %	Element	wt %
C	11.3	Fe	7.8
O	40.3	Si	5.3
Na	6.82	other	2.84
Mg	15.32		
Al	10.23		

Element	wt %	Element	wt %
C	21.1	Fe	2.8
O	45.3	Si	4.3
Na	3.82	S	2.84
Mg	11.32	other	2.29
Al	6.23		

Element	wt %	Element	wt %
C	32.1	Fe	1.1
O	39.3	Si	2.4
Na	3.82	S	4.3
Mg	8.3	N	1.2
Al	3.53	Other	3.95

FIG. 3. SEM micrographs of (**a, b**) LDH dry powder, (**c, d**) LDH, (**e, f**) LDH-SDBS, and (**h, g**) LDH-SDBS after adsorption, the selected area EDS are inserted in (**d**), (**f**), and (**h**). EDS, energy dispersive X-ray spectroscopy; SEM, scanning electron microscope.

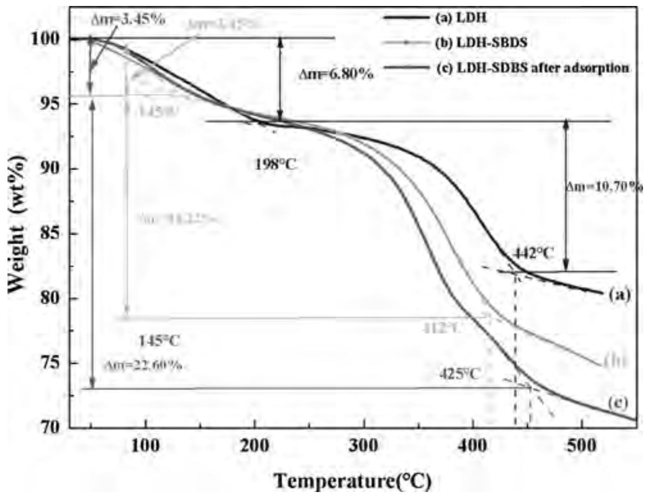

FIG. 4. TG plots of **(a)** LDH, **(b)** LDH-SDBS, and **(c)** LDH-SDBS after adsorption. TG, thermogravimetric.

Sorption kinetic studies

To study the various mechanisms associated with adsorption of organic compounds, two kinetic models were evaluated, namely the pseudo-first-order and the pseudo-second-order (Lagergren, 1989). The linear form of the pseudo-first-order kinetic model is expressed by Equation (3):

$$\log(q_e - q_t) = \log q_e - \frac{K_f}{2.303} t, \tag{3}$$

where K_f (L/min) is the rate constant of pseudo-first-order adsorption and q_e (mg/g) and q_t (mg/g) are the amounts of COD adsorbed at equilibrium and at any time t (min), respectively. The values of K_f and q_e for adsorbate adsorption by LDH-SDBS can be determined from the plot of *log* $(q_e–q_t)$ versus t. The pseudo-second-order equation is expressed as Equation (4) (Ho and McKay 1999):

$$\frac{t}{q_t} = \frac{1}{k_2 q_e^2} + \frac{1}{q_e} t, \tag{4}$$

where k_2 (g/(mg min)) is the pseudo-second-order constant and q_e and k_2 can be determined experimentally from the slope and intercept of the plot t/q_t versus t.

Adsorption thermodynamics

The effect of temperature on adsorption of organic compounds by LDH-SDBS provides clues to determine the thermodynamic parameters: changes of free energy (ΔG), enthalpy (ΔH), and entropy (ΔS) using the Van't Hoff Equations (5)–(7) (Kumar *et al.*, 2008; Eloussaief *et al.*, 2009; Eloussaief and Benzina, 2010; Kannamba *et al.*, 2010; Zhang *et al.*, 2010).

$$K_c = \frac{c_0 - c_e}{c_e} \times \frac{\rho V}{m}, \tag{5}$$

$$\Delta G = -RT \ln K_c, \tag{6}$$

$$\ln K_c = \frac{\Delta S}{R} - \frac{\Delta H}{RT}, \tag{7}$$

where K_c is the distribution coefficient, $\rho = 1$ g/L is the density of the solution mixture, c_e (mg/L) is the COD of the TNT red water treated by LDH-SDBS until equilibrium, q_e is the COD amount of adsorption at equilibrium (mg/g), T is the solution temperature (K), and R is the gas constant and equal to 8.314 J mol/K. ΔH and ΔS are calculated from the slope and intercept of the linear plot of *1/T* versus ln K_c.

Results and Discussion

Formation of LDH with red mud and brucite

The preparation mechanism of LDH using red mud and brurite is discussed hereunder. LDH is prepared with MgO and Al_2O_3 taken from brucite and red mud (Xu and Lu, 2005). Before and during the LDH formation, hydrolysis of MgO and Al_2O_3 in mixed oxides hydrated and dissociation of $Mg(OH)_2$ and $Al(OH)_3$ occurred on the surface of the solid particles as given in the following Equations (8)–(10):

$$MgO + H_2O \leftrightharpoons Mg(OH)_2 \leftrightharpoons Mg^{2+} + 2OH^- \tag{8}$$

$$\begin{aligned} Al_2O_3 + 3H_2O &\leftrightharpoons 2Al(OH)_3 \leftrightharpoons 2Al(OH)_2{}^+ + 2OH^- \\ &\leftrightharpoons 2Al(OH)_2{}^{2+} + 4OH^- \leftrightharpoons 2Al^{3+} + 6OH^- \end{aligned} \tag{9}$$

$$Al(OH)_3 + OH^- \leftrightharpoons Al(OH)_4^- \tag{10}$$

Thin layers of $Mg(OH)_2$ and $Al(OH)_3$ form on the oxide particle surfaces as shown in the first step in Fig. 1 and prevent the inner oxide phase from further hydrolysis. The inside oxide could be further hydrolyzed when the hydroxide layer is dissolved. Therefore, the possible reactions contributing to the LDH formation are shown as given in the following Equations (11)–(13). Formation of LDH by mixed oxides composed of MgO and Al_2O_3 is illustrated as shown in Fig. 1.

$$\begin{aligned} aMg^{2+} + Al(OH)_4{}^- + (2a-2)OH^- + xH_2O + X^- \\ \leftrightharpoons Mg_a\, Al(OH)_{2+2a}X \cdot xH_2O \end{aligned} \tag{11}$$

TABLE 2. BET OF LAYERED DOUBLE HYDROXIDE AND LAYERED DOUBLE HYDROXIDE–SODIUM DODECYL BENZENE SULFONATE BEFORE AND AFTER ADSORPTION

Sample	*Particle size (μm)*	*BET (m²/g)*	*Pore volume (cm³/g)*	*Average pore size (nm)*
LDH	100–650	90.3	0.164	3.412
LDH-SDBS	120–560	78.5	0.113	3.832
LDH-SDBS after adsorption	400–1200	21.7	0.099	2.345

BET, Brunauer-Emmett-Teller; LDH, layered double hydroxide; LDH-SDBS, layered double hydroxide-sodium dodecyl benzene sulfonate.

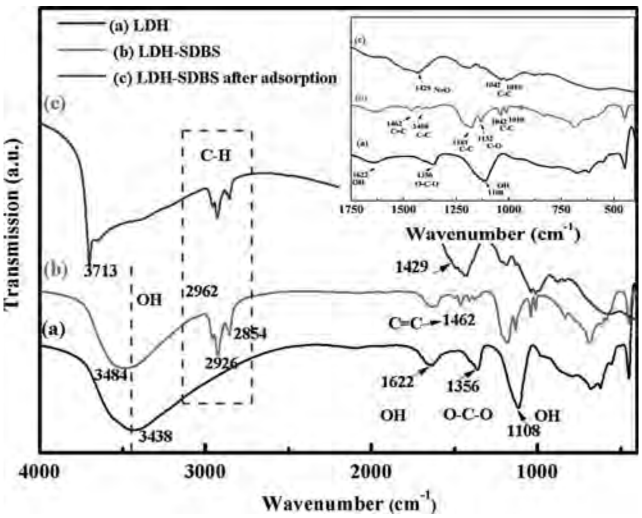

FIG. 5. FT-IR spectra of **(a)** LDH, **(b)** LDH-SDBS, and **(c)** LDH-SDBS after adsorption. FT-IR, Fourier transform infrared.

$$\begin{aligned} &aMg^{2+} + Al(OH)_3 + (2a-1)OH^- + xH_2O + X^- \\ &\leftrightharpoons Mg_a\ Al(OH)_{2+2a}X \cdot xH_2O \end{aligned} \quad (12)$$

$$\begin{aligned} &aMg(OH)_2 + Al(OH)_4^- + xH_2O + X^- \\ &\leftrightharpoons Mg_a\ Al(OH)_{2+2a}\ X \cdot xH_2O + 2OH^- \end{aligned} \quad (13)$$

where X^- denotes OH^-, Cl^-, or 1/2 CO_3^{2-}.

Characterization of samples

XRD, SEM, EDS, TG, N_2 adsorption, and FT-IR were performed to characterize the structure, morphologies, and components of LDH and LDH-SDBS before and after adsorption. Figure 2 shows the XRD patterns of (a) LDH dry powder, (b) LDH, (c) LDH-SDBS, and (d) LDH-SDBS after adsorption. Figure 2A shows that LDH dry powder contains MgO, quartz, calcite, sodalite, and hematite. The XRD peaks at 11.2°, 22.8°, and 34.2° confirm the formation of LDH (Liao *et al.*, 2012). The quartz diffraction peaks are very weak because quartz is dissolved by alkaline solution. The LDH-SDBS peaks shift to smaller angles because of the intercalation of SDBS. After adsorption in TNT red water, the diffraction peaks of LDH-SDBS shift further to smaller angles (Fig. 2B), indicating that the part of organic compounds in TNT red water has been extracted by LDH-SDBS.

SEM shows that the calcined and mixed powders are particles (Fig. 3a, b). The lamellar particles may be the residue of $Mg(OH)_2$. The laminar structures of LDH (Fig. 3c, d) and LDH-SDBS (Fig. 3e, f) indicate that the LDH is prepared with red mud and brucite. Compared with LDH (Fig. 3c, d), LDH-SDBS has irregular shape. After adsorption, a thin layer covers the adsorbent (Fig. 3g, h). EDS (Fig. 3h) shows 1.2% N in LDH-SDBS after adsorption, further proving that the organic compounds in TNT red water have been extracted.

The TG plots of LDH (Fig. 4a) show that the first stage (50°C–198°C) is mainly attributed to elimination of physically adsorbed and interlayer water molecules. The second stage (198°C–442°C) stems from loss of hydroxyl groups from the brucite-like layer along with interlayer carbonate ions followed by destruction of the layered structure. The overall behavior of LDH is in agreement with that reported for MgAl-LDH samples. Figure 4b shows the TG plots of LDH-SDBS, revealing two-step decomposition in SDBS-modified samples in the range 145°C–412°C. However, the weight loss (18.2%) of LDH-SDBS is larger than that of LDH (10.7%). Decomposition of SDBS also takes place during this process and probably interferes with the decomposition of the host materials, especially decomposition of benzene rings and hydrocarbon chains in the absence of free oxygen, which can delay the overall thermal decomposition of the host materials. After adsorption, the TG plots of LDH-SDBS are shown in Fig. 4c. The weight loss of 22.6% of LDH-SDBS after adsorption is larger than those of LDH-SDBS (18.2%) and LDH (6.3%). The larger weight loss is because of adsorption of organic compounds from the TNT red water.

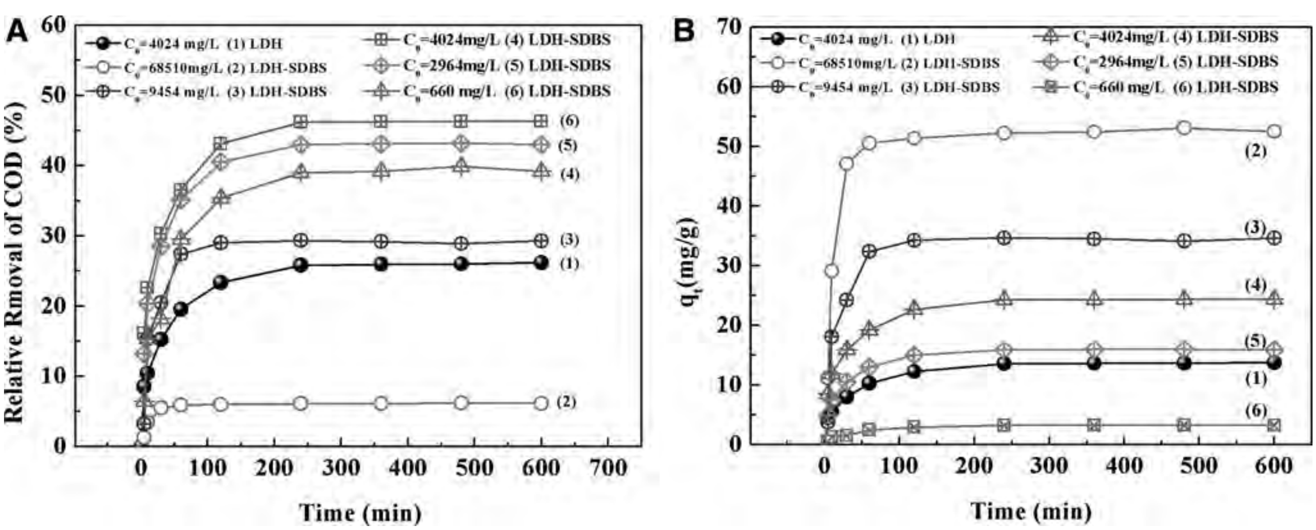

FIG. 6. **(A)** The relative removal of COD at different contact time and initial COD of TNT red water; **(B)** q_t at different contact time and initial COD of TNT red water (adsorbent mass = 4.0 g/50 mL; agitation speed = 150 rpm; T = 298 K). COD, chemical oxygen demand; TNT, 2,4,6-trinitrotoluene.

Table 3. Kinetic Parameters for Adsorption of Organic Compounds of TNT Red Water on LDH-SDBS

			Pseudo-first order			*Pseudo-second order*		
COD_0	T	$q_{e,exp}$	$q_{e,cal}$	k_f	R^2	$q_{e,cal}$	k_2	R^2
68,510	298	51.38	25.16	0.032	0.79651	53.59	0.002	0.99942
9,454	298	34.27	28.90	0.037	0.97723	35.66	0.002	0.99691
4,024	298	22.65	15.80	0.019	0.99339	24.98	0.003	0.99968
4,024	308	23.91	14.20	0.018	0.93601	25.35	0.004	0.99509
4,024	318	27.53	12.19	0.016	0.89017	24.02	0.012	0.99900
4,024	328	28.69	11.58	0.030	0.94973	28.05	0.010	0.99957
4,024	338	28.95	10.72	0.028	0.92314	27.99	0.012	0.99975
2,964	298	15.01	10.82	0.021	0.99089	16.38	0.005	0.99972
660	298	2.92	2.67	0.019	0.97813	3.42	0.012	0.99856

COD_0 (mg/L), T (K), $q_{e,exp}$ (mg/g), $q_{e,cal}$ (mg/g), k_f (L/min), k_2 (g/(mg min)).
COD, chemical oxygen demand; TNT, 2,4,6-trinitrotoluene.

When the temperature goes up, the organic species break down, leading to higher weight loss (Zhao *et al.*, 2002).

Surface area, pore size, and pore volume of LDH and LDH-SDBS before and after adsorption are measured by N_2 adsorption. The Brunauer-Emmett-Teller (BET) of LDH is 90.3 m^2/g, pore volume is 0.164 cm^3/g, and average pore size is 3.412 nm as shown in Table 2. After LDH is modified by SDBS, the BET and pore volume of LDH-SDBS decline slightly because of the adsorption of SDBS on the surface of LDH. After adsorption, the BET, pore volume, and average pore size of LDH-SDBS decrease further because of the attachment of organic pollutants from TNT red water. The smaller pore size and volume show that organic species are adsorbed effectively by LDH-SDBS.

FT-IR spectra (Fig. 5) show the functional groups of (a) LDH, (b) LDH-SDBS, and (c) LDH-SDBS after adsorption. The broad and strong absorption band at 3438 cm^{-1} is attributed to stretching vibrations of physically adsorbed water, structural OH group, and/or hydrogen-bonded hydroxyl group (OH-OH). The band at 1,622 cm^{-1} corresponds to bending mode of interlayer water molecules. The sharp intense band at 1,356 cm^{-1} is assigned to O-C-O stretching vibrations of monodentate carbonate species (Iglesias *et al.*, 2005). The FT-IR spectrum of LDH-SDBS shows new peaks at 2,962, 2,926, and 2,854 cm^{-1} assigned to C-H stretching vibrations of SDBS. Moreover, the characteristic peaks of C=C and C-C at 1,462 cm^{-1} and 1,408 cm^{-1} are observed (He *et al.*, 2004), illustrating that LDH is modified by SDBS. After adsorption, the C-H stretching vibrations peaks of SDBS at 2,962, 2,926, and 2,854 cm^{-1} still exist except the peaks of $N=O$ at 1,429 cm^{-1}, indicating that the organic materials are adsorbed by LDH-SDBS.

Table 4. Thermodynamic Parameters for Adsorption of Organic Compounds of TNT Red Water on Layered Double Hydroxide-Sodium Dodecyl Benzene Sulfonate

	Temperature (K)				
Parameters	*298*	*308*	*318*	*328*	*338*
K_c	9.48	10.44	13.76	15.03	15.34
ΔG (kJ/mol)	−5.57	−6.01	−6.93	−7.39	−7.67
ΔH (kJ/mol)			11.20		
ΔS (J/(mol K))			56.34		

Adsorption kinetics of organic components on LDH-SDBS

Adsorption of organic components of TNT red water occurs very quickly at the beginning of the experiments (Fig. 6) and slows gradually after 60 min. The adsorption processes reach equilibrium at 240 min. LDH-SDBS possesses higher adsorption ability than LDH (Fig. 6A). At the same initial concentration of TNT red water (4,024 mg/L), the COD removal efficiency increases from 26% to 46% and final COD of TNT red water decreases from 4,024 to 2,253 mg/L. Figure 6B shows that q_t of LDH-SDBS at equilibrium increases from 3.2 to 52 mg/g with increasing initial COD, whereas COD removal efficiency decreases from 46% to 6%. The initial COD of TNT red water plays an important role in adsorption on LDH-SDBS. It can be explained by that rapid adsorption during initial exposure arises from the availability of physisorbed molecules of SDBS on the LDH-SDBS. The slow rate of organic components adsorption later is probably because of gradual penetration through the pores in the interior surfaces and interlayer of LDH-SDBS as the exterior became saturated (Pavan *et al.*, 2000; Eloussaief *et al.*, 2011; Eloussaief *et al.*, 2013).

Both kinetic models fit the experimental data well (Table 3), but the pseudo-second-order model provides the best overall

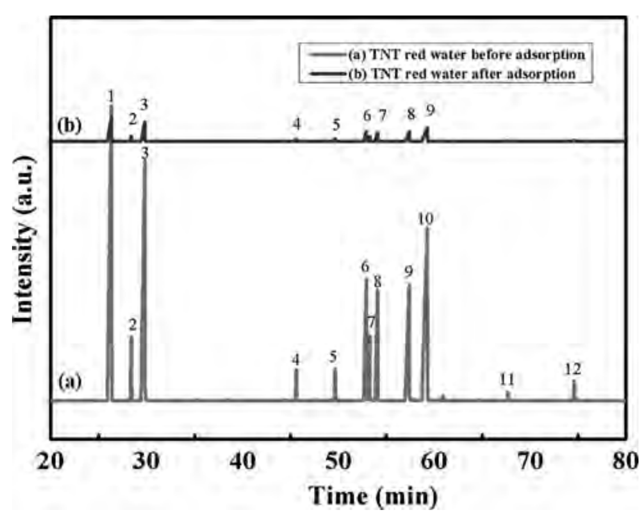

FIG. 7. Gas chromatography of TNT red water before **(a)** and after **(b)** adsorption on LDH-SDBS.

fit and the calculated $q_{e,cal}$ with this model is consistent with the experimental value $q_{e,exp}$. It suggests that pseudo-second-order adsorption is predominant (Mandal *et al.*, 2014).

Thermodynamics adsorption of organic components on LDH-SDBS

The thermodynamic parameters are calculated and the slope and the intercept are shown in Table 4. ΔG is less than 0 (kJ/mol) (–5.57, –6.01, –6.93, –7.39, and –7.67) under the experimental conditions, indicating that adsorption of organic species is spontaneous. The increasingly negative ΔG with increasing temperature implies that adsorption becomes more favorable at higher temperatures. The positive ΔH indicates that adsorption on the LDH-SDBS is endothermic, suggesting that a higher temperature increases the number of adsorption sites on LDH-SDBS. In general, uptake of solutes from an aqueous solution by a solid sorbent has the following mechanisms: physisorption and chemisorption. This classification is based on ΔH during the mass transfer process. If the interaction between the solute and sorbent is based on chemical bonding, ΔH is greater than 40 kJ/mol. Here, ΔH (11.20 kJ/mol) is between 2 and 40 kJ/mol, thus indicating physical adsorption (Eloussaief *et al.*, 2012; Yang *et al.*, 2014). TNT red water has water as a solvent. Adsorption of organic compounds from TNT red water by LDH-SDBS displaces water molecules, and the entropy change ΔS of water molecules desorption is greater than that of organic compounds, being consistent with an increase in randomness during adsorption (Zheng *et al.*, 2008).

Compounds in TNT red water

GC/MS (Fig. 7 and Table 5) shows some organic species such as 4-methyl-2,6-dinitro-phenol, 5-nitro-1H-indazole, and 3,5-dinitro *p*-toluidine cannot be detected and so they have been removed. In addition, the acute toxicity tests before and after treatment have been conducted by Zhang *et al.* (2011) and the acute toxicity of TNT red water is greatly reduced compared with that of the unprocessed TNT red water (Zhang *et al.*, 2011).

Cost analysis

Sorption cost of COD for activated carbon, activated coke (Zhang *et al.*, 2011), bamboo charcoal (Fu *et al.*,), RS-50B, bentonite (Zhang *et al.*, 2014), and LDH-SDBS to TNT red water is compared in Table 6. Based on this analysis, the sorption capacity of RS-50B is the largest. In addition, the

Table 5. GC/MS Results of the TNT Red Water Before and After Adsorption

TNT red water before adsorption				TNT red water after adsorption			
Peaks	*Retention time (minutes)*	*Relative content (%)*	*Compound*	*Peaks*	*Retention time (minutes)*	*Relative content (%)*	*Compound*
1	26.3	26.28	Benzene, 1-methyl-2-nitro-	1	26.1	6.3	Benzene, 1-methyl-2-nitro-
2	28.4	2.14	Benzene, 1-methyl-3-nitro-	2	28.4	0.18	Benzene, 1-methyl-3-nitro-
3	29.8	21.15	Benzene, 1-methyl-4-nitro-	3	29.8	1.90	Benzene, 1-methyl-4-nitro-
4	45.6	0.98	Benzene, 2-methyl-1,3-dinitro-	4	45.6	0.09	Benzene, 2-methyl-1,3-dinitro-
5	49.7	1.12	Benzene, 1-methyl-2,4-dinitro-	5	49.7	0.13	Benzene, 1-methyl-2,4-dinitro-
6	52.9	8.02	3-Methyl-6-nitrobenzoic acid	6	52.9	1.02	3-Methyl-6-nitrobenzoic acid
7	53.3	3.32	Phenol, 4-methyl-2,6-dinitro-	7	54.1	0.82	Phenol, 2-methyl-4,6-dinitro-
8	54.1	6.19	Phenol, 2-methyl-4,6-dinitro-	8	57.4	10.01	Phenol, 4-methyl-2,6-dinitro-
9	57.4	10.01	Phenol, 4-methyl-2,6-dinitro-	9	59.3	1.97	1,3,5-Trinitrobenzene
10	59.3	19.07	1,3,5-Trinitrobenzene				
11	64.8	0.27	1H-Indazole, 5-nitro-				
12	74.6	0.78	*p*-Toluidine, 3,5-dinitro				

GC/MS, Gas Chromatography-Mass Spectrometer.

Table 6. Costs of Different Adsorbents for TNT Red Water

Adsorbent	*Sorption capacity (mg COD/g)*	*Price (CNY/kg)*	*Sorption cost (CNY/g COD)*
Activated carbon	10.4	10	0.96
Activated coke	60.5	0.5	0.0083
Bamboo charcoal	31.77	1.3–1.9	0.041–0.06
RS-50B	136.00	45	0.33
Bentonite	45.4	1–1.2	0.022–0.026
LDH-SDBS	52.00	0.6–0.8	0.012–0.015

sorption cost of activated coke was a little higher than that of LDH-SDBS. However, the cost of RS-50B is 45 China Yuan (CNY)/kg, which is much higher than that of LDH-SDBS. The sorption cost for LDH-SDBS is only 0.012–0.015 CNY/g COD, which is much lower than that of RS-50B, activated carbon, bamboo charcoal, and bentonite and slightly higher than that of activated coke. According to the analysis of these adsorbents, it can be concluded that LDH-SDBS is an inexpensive and effective absorbent for the treatment of TNT red water.

Conclusions

LDH-SDBS prepared from brucite and red mud shows large potential pertaining to the removal of organic compounds from TNT red water. The COD of TNT red water is reduced from 4,024 to 2,253 mg/L and removal efficiency reaches 46%. The adsorption kinetics of COD removal from TNT red water fit the pseudo-second-order kinetic model. Thermodynamic analyses indicate that adsorption is endothermic and spontaneous and GC/MS results show that most organic compounds were removed by LDH-SDBS. Compared with that of other adsorbents, the sorption cost of LDH-SDBS is quite low at 0.012–0.015 CNY/g COD.

Acknowledgments

We thank the following funding sources for generously supporting this research: the Fundamental Research Funds for the Central Universities (2010ZD08), National High Technology Research and Development Program (863 Program 2012AA06A109) of China, and City University of Hong Kong Applied Research Grant (ARG) No. 9667122.

Author Disclosure Statement

No competing financial interests exist.

References

Ayoub, K., Hullebusch, E.D.V., Cassir M., and Bermond, A. (2010). Application of advanced oxidation processes for TNT removal: A review. *J. Hazard. Mater.* 178, 10.

Basile, F., Basini, L., Amore, M.D., Fornasaria, G., Guarinonib, A., Matteuzzia, D., Pieroc, G.D., Trifiròa, F., and Vaccaria, A. (1998). Ni/Mg/Al anionic clay derived catalysts for the catalytic partial oxidation of methane: Residence time dependence of the reactivity features. *J. Catal.* 173, 247.

Bontchev, R.P., Liu, S., Krumhansl, J.L., Voigt, J., and Nenoff, T.M. (2003). Synthesis, characterization, and Ion exchange properties of hydrotalcite $Mg_6Al_2(OH)_{16}(A)_x(A')_{2-x}\cdot 4H_2O$ (A, A' = Cl^-, Br^-, I^-, and NO_3^-, $2 \geq x \geq 0$) Derivatives. *Chem. Mater.* 15, 3669.

Braterman, P.S., Xu, Z.P., and Yarberry, F. (2004). Layered double hydroxides (LDHs). *Cheminform* 36, 907.

Eloussaief, M., and Benzina, M. (2010). Efficiency of natural and acid-activated clays in the removal of Pb(II) from aqueous solutions. *J. Hazard. Mater.* 178, 753.

Eloussaief, M., Fakhfakh, N., and Sdiri, A. (2012). An experimental design for the optimization of brick manufacturing procedure: Application on the late miocene clays, Southern Tunisia. *T. Indian Ceram. Soc.* 71, 195.

Eloussaief, M., Hamza, W., Kallel, N., and Benzinaa, M. (2013). Wastewaters decontamination: Mechanisms of PB(II), ZN(II), and CD(II) competitive adsorption on tunisian smectite in single and multi-solute systems. *Environ. Prog. Sustain. Energy* 32, 229.

Eloussaief, M., Jarraya, I., and Benzina, M. (2009). Adsorption of copper ions on two clays from Tunisia: pH and temperature effects. *Appl. Clay Sci.* 46, 409.

Eloussaief, M., Kallel, N., Yaacoubi, A., and Benzinaa, M. (2011). Mineralogical identification, spectroscopic characterization, and potential environmental use of natural clay materials on chromate removal from aqueous solutions, *Chem. Eng. J.* 168 1024.

Evans, D.G., and Slade, R.C.T. (2006). *Structural Aspects of Layered Double Hydroxides*. Springer Berlin Heidelberg, 119, 1.

Fu, D., Zhang, Y.H., Lv, F.Z., Chu, K.P., and Shang, J.W. (2012). Removal of organic materials from TNT red water by Bamboo Charcoal adsorption, *Chem. Eng. J.* 193, 39.

He, H.P., Ray, F.L., and Zhu, J.X. (2004). Infrared study of HDTMA+ intercalated montmorillonite. *Spectrochim. Acta Part A* 60, 2853.

Ho, Y.S., and McKay, G. (1999). Pseudo-second order model for sorption processes. *Process Biochem.* 34, 451.

Hu, P., Zhang, Y.H., Lv, F.Z., Wang, X.K., Wei, F.F., Meng, X.H., and Jiang, S.B. (2014). Organic compounds removal from TNT red water using Cu-impregnated activated coke. *Water Air oil Pollut.* 225, 1.

Hu, P., Zhang, Y.H., Tong, K., Wei, F.F., An, Q., Wang, X.K., Chu, K.P., and Lv, F.Z. (2015). Removal of organic materials from red water by magnetic activated coke. *Desalin. Water Treat.* 54, 2710.

Hwang, S., Bouwer, E.J., Larson, S.L., and Davis, J.L. (2004). Decolorization of alkaline TNT hydrolysis effluents using UV/H2O2. *J. Hazard. Mater.* 108, 61.

Iglesias, A.H., Ferreira, O.P., Gouveia, D.X., Filho, A.G.S., Paiva, J.A.C.D., Filho, J.M., and Alves, O.L. (2005). Structural and thermal properties of Co-Cu-Fe hydrotalcite-like compound. *J. Solid State Chem.* 178, 142.

Jo, J.H., Ernest, T., and Kim, K.J.(2014). Treatment of TNT red water by layer melt crystallization. *J. Hazard. Mater.* 280, 185.

Kannamba, B., Reddy, K.L., and AppaRao, B.V., (2010). Removal of Cu (II) from aqueous solutions using chemically modified chitosan. *J Hazard. Mater.* 175, 939.

Kumar, A., Prasad, B., and Mishra, I.M. (2008). Adsorptive removal of acrylonitrile by commercial grade activated carbon: Kinetics, equilibrium and thermodynamics. *J. Hazard. Mater.* 152, 589.

Lagergren, S. (1898). About the theory of so called adsorption of soluble substances. *Ksver. Veterskapsakad. Handl.* 24, 1.

Li, Y.M., Gu, G.W., Zhao, J.F., Yu, H.Q., Qiu, Y.L., and Peng, Y.Z. (2003). Treatment of coke-plant wastewater by biofilm systems for removal of organic compounds and nitrogen. *Chemosphere* 52, 997.

Liao, L.B., Zhao, N., and Xia, Z.G. (2012). Hydrothermal synthesis of Mg-Al layered double hydroxides (LDHs) from natural brucite and Al(OH)3. *Mater. Res. Bull.* 47, 3897.

Ludwichk. R., Helferich, O.K., Kist, C. P., Lopesa, A.C., Cavasottoa, T., Silvab, D.C., and Barreto-Rodriguesa, M. (2015). Characterization and photocatalytic treatability of red water from Brazilian TNT industry. *J Hazard. Mater.* 293, 81.

Mandal, S., Sahu, M.K., Giri, A.K., and Patel, P.K. (2014). Adsorption studies of chromium (VI) removal from water by lanthanum diethanolamine hybrid material. *Environ. Technol.* 35, 817.

Matta, R., Hanna, K., Kone, T., and Chiron, S. (2008). Oxidation of 2,4,6-trinitrotoluene in the presence of different ironbearing minerals at neutral pH. *Chem. Eng. J.* 144, 453.

Meng, Q.Q., Song, K., Zhao, Q.L., and Ye, Z.F. (2013). Removal of nitro aromatic compounds and sulfite acid from distillate of 2, 4, 6-trinitrotoluene red water using modified porous polystyrene microspheres. *J. Appl. Poly. Sci.* 127, 1578.

Meng, Q.Q., Zhao, Q.L., Zhao, X., Wu, T., and Ye, Z.F. (2012). Removal of nitro aromatic compounds from 2,4,6-Trinitrotoluene red water using 1,2-Ethanediamine modified macroporous polystyrene microspheres. *Clean-Soil Air Water* 40, 823.

Nakayama, H., Wada N., and Tsuhako, M. (2004). Intercalation of amino acids and peptides into Mg-Al layered double hydroxide by reconstruction method. *Int. J. Pharm.* 269, 469.

Nefso, E.K., Burns, S.E., and McGrath, C.J. (2005). Degradation kinetics of TNT in the presence of six mineral surfaces and ferrous iron. *J. Hazard. Mater.* 123, 79.

Park, C., Kim, T.H., Kim, S., Kim, S.W., Lee, J., and Kim, S.H. (2003). Optimization for biodegradation of 2,4,6-trinitrotoluene (TNT) by Pseudomonas putida. *J. Biosci. Bioeng.* 95, 567.

Pavan, P.C., Crepaldi, E.L., and Valim, J.B. (2000). Sorption of anionic surfactants on layered double hydroxides. *J. Colloid Interface Sci.* 229, 346.

Shen, B., Zhang, Y.H., An, Q., Yu, L., and Shang, J.W. (2014). Cu_2O immobilized on reduced graphene oxide for the photocatalytic treatment of red water produced from the manufacture of TNT. *Desalin. Water Treat.* 54, 1.

Stanimirova, T., and Balek, V. (2008). Characterization of layered double hydroxide Mg-Al-CO3 prepared by re-hydration of Mg-Al mixed oxide. *J. Ther. Anal. Calorim.* 94, 477.

Wei, F.F., Zhang, Y.H., Lv, F.Z., and Chu K.P. (2011). Extraction of organic materials from red water by metal-impregnated lignite activated carbon. *J. Hazard. Mater.* 197, 352.

Xu Z P, and Lu G Q. (2005). Hydrothermal synthesis of Layered Double Hydroxides (LDHs) from mixed MgO and Al2O3: LDH Formation Mechanism[J]. *Chem. Mater.* 17, 1055.

Yang, J, Yu M., and Qiu, T. (2014). Adsorption thermodynamics and kinetics of Cr(VI) on KIP210 resin. *J. Ind. Eng. Chem.* 20, 480.

Zhang, M.H., Liu, G.H., Song, K., Wang, Z.Y., Zhao, Q.L., Li, S.J., and Ye, Z.F. (2015). Biological treatment of 2,4,6-trinitrotoluene (TNT) red water by immobilized anaerobic–aerobic microbial filters. *Chem. Eng. J.* 259, 876.

Zhang, M.H., Zhao Q.L., and Ye, Z.F. (2011). Organic pollutants removal from 2, 4, 6- trinitrotoluene (TNT) red water using low cost activated coke. *J. Environ. Sci.* 23, 1.

Zhang, Q., Meng, Z.L., Zhang, Y.H., Lv, G.C., Lv, F.Z., and Wu, L.M. (2014). Modification of a Na-montmorillonite with quaternary ammonium salts and its application for organics removal from TNT red water, *Water Science & Technology.* 69, 1798.

Zhang, X., Lin, Y.M., Shan, X.Q., and Chen Z.L. (2010). Degradation of 2, 4, 6-trinitrotoluene (TNT) from explosive wastewater using nanoscale zero-valent iron, *Biochemical Engineering Journal.* 158 566.

Zhao, Q.L., Gao, Y.C., and Ye, Z.F. (2013). Reduction of COD in TNT red water through adsorption on macroporous polystyrene resin RS 50B, *Vacuum.* 95, 71.

Zhao, Q.L., Ye, Z.F., and Zhang, M.H. (2010). Treatment of 2,4,6-trinitrotoluene (TNT) red water by vacuum distillation, *Chemosphere.* 80, 947.

Zhao, Y., Li, F., Zhan, R., Evans, D.G., and Duan, X. (2002). Preparation of layered double-hydroxide nanomaterials with a uniform crystallite size using a new method involving separate nucleation and aging steps. *Chem. Mater.* 14 4286.

Zheng, H., Han, L.J., Ma, H.W., Zheng, Y., Zhang, H.M., Liu, D.H., and Liang, S. (2008). Adsorption characteristics of ammonium ion by zeolite 13×. *J. Hazard. Mater.* 158, 577.

Zhi, P.X., and Guo, Q.L. (2005). Hydrothermal Synthesis of Layered Double Hydroxides (LDHs) from Mixed MgO and Al_2O_3: LDH Formation Mechanism. *Chem Mater.* 17, 1055.

Zhu, Q.W., Zhang, Y.H., Zhou, F.S., Lv, F.Z., Ye, Z.F., and Chu, K.P. (2011). Preparation and characterization of Cu_2O–ZnO immobilized on diatomite for photocatalytic treatment of red water produced from manufacturing of TNT. *Chem. Eng. J.* 171, 61.